JOURNAL OF GEOPHYSICAL RESEARCH, VOL. 100, NO. C11, PAGES 22,591–22,601, NOVEMBER 15, 1995

The absolute velocity field of Agulhas eddies and the Benguela Current

Amy C. Clement and Arnold L. Gordon

Lamont-Doherty Earth Observatory, Palisades, New York

Abstract. Acoustic Doppler current profiler (ADCP) data referenced to Global Positioning System navigation were obtained in May 1993 from the Royal Research Ship*Discovery* within the Benguela Current as part of the Benguela Source and Transport (BEST) project. These data are used in combination with hydrographic data collected during the cruise to investigate the absolute geostrophic velocities in the Benguela Current and the transient eddies. Four anticyclonic eddies were encountered during the cruise, of which three were determined to be Agulhas Retroflection eddies of various ages and one was determined to be an eddy derived from the Brazil Current. ADCP velocities averaged between conductivity-temperature-depth stations have a high linear correlation with geostrophic velocities derived from the hydrographic data (correlation coefficient of 0.93) along the entire cruise track. The magnitudes of the two velocity estimates, however, were notably different within the eddies. It was determined that these discrepancies are probably due to a significant barotropic component of the flow near the eddy center. As much as 50% of the total flow in the eddy is barotropic. The horizontal length scale (radius of maximum velocity) of this eddy determined from both the ADCP data and the thermal field was found to be approximately 60 km, considerably smaller than previous estimates, which are about 120 km. The barotropic component in Agulhas eddies leads to an equal partitioning of total mechanical energy between available potential and kinetic energy. It is also expected to have a significant effect on the climatically important exchange of mass between the Indian and South Atlantic Oceans. Total geostrophic velocities were computed for the Benguela Current using the averaged ADCP at 250 m as a reference. The ADCP referenced geostrophic transport across 30°S of water warmer than 9°C in the Benguela Current was found to be 17 Sv (1 Sv= 10^6 m^3 s^{-1}) to the north and that of the upper kilometer was 25 Sv to the north. These values are largely consistent with previous estimates, suggesting that the upper layer flow across this section is dominated by the baroclinic field.

1. Introduction

The water mass composition of the Benguela Current reflects its varied origins [*Stramma and Peterson*, 1989]. As the eastern limb of the subtropical gyre of the South Atlantic, the Benguela Current is fed by the South Atlantic Current with significant input of Indian Ocean thermocline water [*Gordon*, 1985, 1986; *Gordon et al.*, 1992]. This interocean exchange arises from the complex nature of the Agulhas Retroflection within the Benguela Current source region.

The southern terminus of the African continent lies at a lower latitude than the maximum westerlies. Therefore the western boundary current of the Indian Ocean, the Agulhas Current, follows a westward path along the continental margin to the southern limits of Africa, allowing for the possibility of penetration into the South Atlantic. Near 20°E the current separates from the continent where it undergoes an abrupt anticyclonic turn and flows eastward back into the Indian Ocean. This circulation feature, known as the Agulhas Retroflection, occurs consistently, although the longitude at which it takes place has been observed to vary between 16° and 20°E [*Lutjeharms and van Ballegooyen*, 1988]. Satellite observations of the Agulhas Retroflection reveal warm core eddies being spawned at its western end at rates between five and seven eddies per year [*Gordon and Haxby*, 1990; *Byrne et al.*, 1995; *van Ballegooyen et al.*, 1994]. *Feron et al.* [1992] show that this rate is probably highly variable but is, on average, six per year. These eddies enclose a pool of Indian Ocean water from the Agulhas current which is modified through contact with the atmosphere both within the retroflection and the eddies [*Olson et al.*, 1992]. In the absence of a western continental barrier, Agulhas eddies can migrate well into the South Atlantic [*Byrne et al.*, 1995; *McCartney and Woodgate-Jones*, 1991], carrying with them heat, salt, and vorticity from the Indian Ocean. In addition, filaments and plumes of water from the Agulhas Retroflection have been observed to pass into the South Atlantic [*Lutjeharms and Cooper, 1995*]. While Indian ocean water is sporadically drawn into the Benguela Current source region via such mechanisms, South Atlantic water advected with the South Atlantic Current (SAC) feeds into the Benguela Current as the SAC turns northward and separates from the Subtropical Front [*Stramma and Peterson*, 1990]. Also, water from the subantarctic is advected into the region in association with Agulhas eddies which direct high-speed jets around their

Paper number 95JC02421.
0148-0227/95/95JC-02421$05.00

peripheries [*Shannon et al.*, 1989; *Lutjeharms and van Ballegooyen*, 1988]. This situation leads to a complex blending of the water masses in the source region of the Benguela Current, which is subsequently exported out of the region to the north (roughly) by the Benguela Current, while Indian Ocean water is exported to the west by the Agulhas eddies that escape out of the region.

The presence of Indian Ocean thermocline water in the South Atlantic has important climatic implications. The modification that the Indian Ocean water undergoes in the southeastern corner of the South Atlantic leaves a positive salinity anomaly [*Olson et al.*, 1992] which may affect the salt budget of the South Atlantic and ultimately the formation of North Atlantic Deep Water (NADW) [*Gordon*, 1986]. It is thus desirable to constrain the property fluxes associated with this interocean exchange. However, it is difficult to determine the climatic-scale transport, as the exchange is carried out by processes that occur on shorter timescales. While eastern boundaries in the ocean are typically quiescent regimes, the southeastern corner of the South Atlantic is shown by satellite imagery to have the highest mesoscale variability of the entire southern hemisphere [*Gordon and Haxby*, 1990, Plate 1]. Estimates of the Indian to South Atlantic exchange from different studies range between 2 and 19 Sv (1 Sv = 10^6 m^3 s^{-1}). Although this variability may be the result of artifacts in the different methods, it may well be real variability due to the transient nature of the processes that carry out the exchange [*Gordon et al.*, 1992].

The Benguela Source and Transport (BEST) project was designed to investigate the processes in the source region of this current that lead to the injection of Indian Ocean water into the South Atlantic and the form of the Benguela Current which carries the melange of waters out of the region to the north. The field work consisted of conductivity-temperature-depth(CTD) casts and mooring deployments. There were three BEST cruises which were carried out between June 1992 and November 1993. The first and third legs involved the deployment and recovery of moorings. The second leg was aboard the Royal Research Ship (RRS) *Discovery* cruise 202. Its main activity was a comprehensive CTD survey. The *Discovery* was equipped with a hull-mounted acoustic Doppler current profiler (ADCP). The combination of the CTD survey and the ADCP provides an opportunity to define the absolute velocity field of the Benguela Current and the eddies. This aspect of the *Discovery* cruise 202 is presented here. In particular, this study will focus on the contribution of Agulhas eddies to the Indian to South Atlantic exchange through an investigation of the basic structure of the eddies (which is important in determining their transport, evolution, and trajectories), as well as on the velocity structure of the Benguela Current. A more detailed analysis of the water masses will be presented in a later paper.

2. The *Discovery* Cruise 202 Data Set

We The *Discovery* cruise 202 was carried out in May 1993. Data from 69 CTD stations were collected with a Neil Brown Mk III unit, and five CTD stations were completed with a Sea-Bird unit. Bottom-reaching casts were obtained along two lines of moorings (Figure 1), and casts reaching a nominal

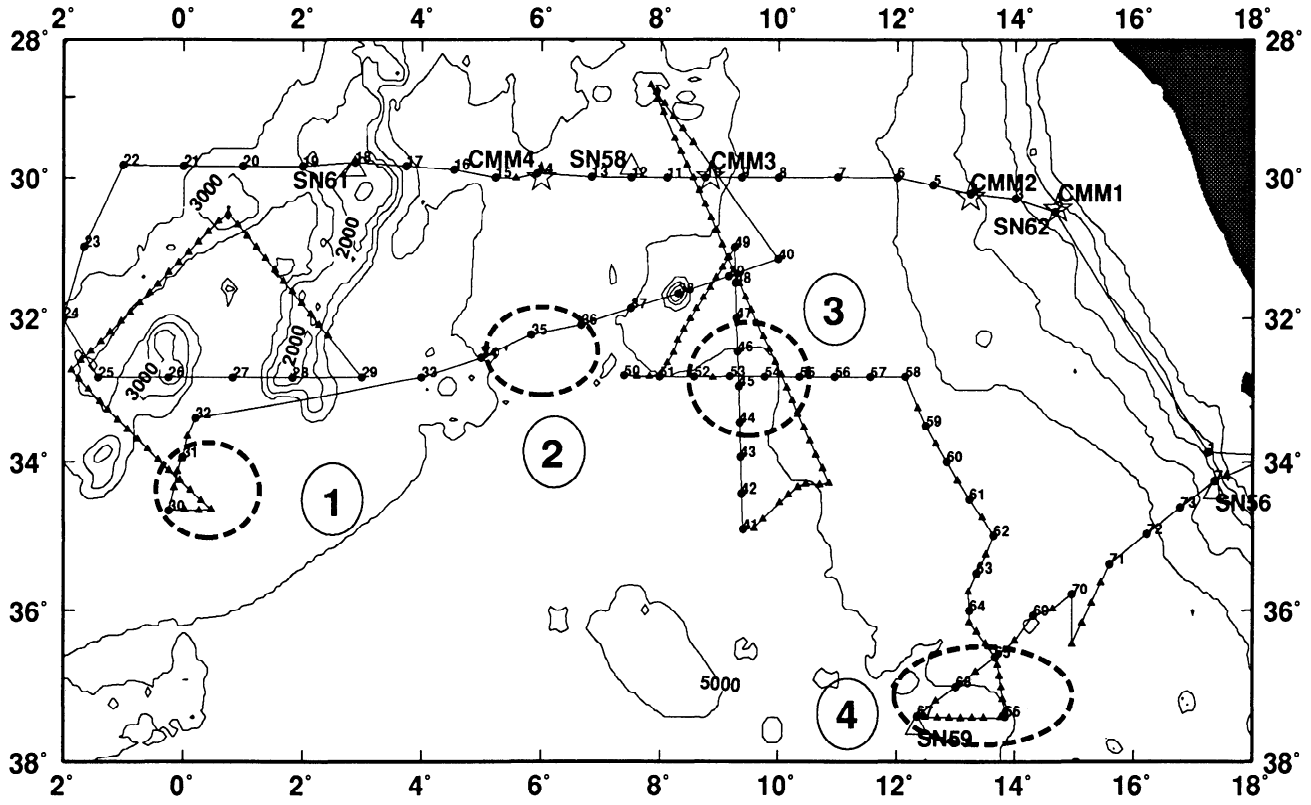

Figure 1. RRS *Discovery* voyage 202 cruise track, conductivity-temperature-depth (CTD) stations (solid circles), expendable bathythermographs (XBTs) (solid triangles), and contours of the bottom depth in meters. Current meter moorings (CMMs) and inverted echo sounder (SN) from the two other Benguela Source and Transport Project (BEST) cruises are shown by stars and open triangles, respectively. The approximate locations of the eddies encountered during the *Discovery* 202 cruise are indicated by the dashed circles and are numbered.

depth of approximately 1500 dbar were obtained along the rest of the cruise track. Water samples were collected with a 24-bottle, 1.7-L rosette system for CTD calibration. In addition, 144 expendable bathythermograph (XBT) probes were launched to provide views of the thermal structure along the track down to approximately 800 m. Surface salinity was also monitored using the SeaCat CTD placed in a bucket filled with a running stream of water from the ship's uncontaminated seawater supply. TOPEX/POSEIDON satellite altimeter data were used prior to the cruise to provide a target for the eddy search. A real-time data stream of ADCP velocities was used to determine when an eddy was being encountered, at which point the XBT surveys were performed to explore the thermal structure of the features. This should explain the somewhat erratic character of the cruise track (Figure 1). With the navigation control provided by Global Positioning System (GPS) navigation available throughout the cruise, high-quality ADCP data were obtained with the ship's RD Instruments unit. The ADCP was set to average data in 16 m depth bins at two-min intervals. The quality of the acoustic signal was high down to a depth of approximately 300 m below which it degraded rapidly.

In the past the overwhelming source of instrumental error in the ADCP velocities was associated with a lack of good navigation control. This source of error is virtually eliminated through use of the GPS system. The currents logged by the ADCP were corrected for the ship's motion by taking the vector difference between the measured velocities and the ship velocity as determined by smoothed GPS positions. One source of instrumental error may arise if the ADCP instrument is not aligned with the ship. This error can be estimated by comparing the ADCP velocities derived using bottom-tracking navigation and those using GPS navigation, and this was done at the start of the *Discovery* cruise 201. The error in the ship's heading was found to be -0.5°. Previous estimates of the misalignment on the *Discovery* are given by *Saunders and King* [1995] and are roughly the same (about -0.6°). This results in a small error (1-2 cm s^{-1}) in the averaged ADCP velocities [*Saunders and King* , 1995, Table 3]. Another source of instrumental error can arise because of gaps in the GPS navigation. Thus the GPS positions were smoothed over an interval of 2 min, and the velocities were averaged over this time rather than between successive position fixes. Therefore the data collected while coming into station and at the stations, as well as other periods during which the ship's heading varied rapidly, were not used in the analysis.

Prominent features of the circulation in the region of the cruise track are revealed from both the topography of the thermocline, which provides a plausible depiction of the baroclinic field [*Gordon et al.*, 1987], and the averaged ADCP data. We use the depth of the 10°C isotherm as a proxy for the thermocline topography because of its high linear correlation (0.96) with the dynamic height computed relative to 1000 dbar (Figure 2). Use of the 10°C isotherm allows a much higher spatial resolution of the baroclinic field than the CTD data alone. The topography of the 10°C isotherm and the ADCP vectors at 250 m are in close agreement (Figure 3). Disagreement between the two may arise where there is either a barotropic or an ageostrophic component to the flow.

Four anticyclonic eddies were encountered during the *Discovery* cruise 202. Eddy 1 (Figure 1) was centered at approximately 0° longitude and 34°S latitude. The core temperature was 13°C, and the salinity was approximately 35.2 parts per thousand (Figure 4), which is about 0.2 above

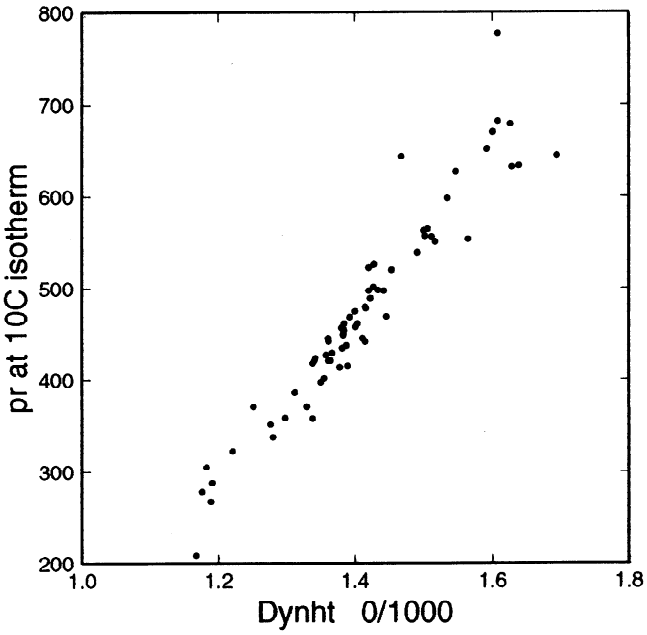

Figure 2. Pressure of the 10°C isotherm (decibars) versus the dynamic height of the sea surface relative to 1000 dbar (dynamic centimeters).

the regional salinity at that temperature. Because the Agulhas Retroflection encloses a pool of approximately 17-18°C South Indian subtropical mode water [*Olson et al.*, 1992], the much cooler core temperature of this feature indicates that it may not be an Agulhas Retroflection eddy. Indeed, previous observations aboard the *Discovery* cruise 199 in January 1993 showed levels of CFC-11 and CFC-113 for this same eddy that suggest an age of 4.5 years [*Smythe-Wright et al.*, 1995. This age may be greater than the actual age of the eddy because in a convective mixed layer, the water trapped within the eddy core experiences entrainment of deeper, older water; that is, the mixed layer is not "up-to-date" and is below equilibrium saturation (D. Olson, personal communication, 1995). *Smythe-Wright et al.* [1995] concluded that the feature was a Brazil Current eddy that had presumably traveled eastward across the South Atlantic with the South Atlantic Current and then migrated northward as it turned back toward the west. Subsequently, other likely Brazil eddies have been identified in the Cape Basin [*Duncombe Rae et al.*, 1995]. The center of eddy 1 was determined from the thermal field (Figure 3), and azimuthal velocities were computed from the ADCP (averaged over 15 min intervals) at 250 m from around eddy 1. These velocities are superimposed on one radius and smoothed with a 10-point running mean (Figure 5). The maximum velocity occurs at a radius of approximately 60 km, where the unsmoothed azimuthal velocity was approximately 45 cm s^{-1}.

Eddy 2 (Figure 1) was located at approximately 6°E and 32°S. This eddy had a core temperature of 15-16°C, slightly below that of Agulhas Retroflection water, and positive salinity anomaly of about 0.2 part per thousand (Figure 4). These properties suggest that this feature is an Agulhas eddy which has been cooled and ventilated under winter conditions [*Olson et al.*, 1992], although *Walker and Mey* [1988] show that Agulhas eddies can lose heat to the atmosphere during summer as well . The positive salinity anomaly is induced as heat is removed from the eddy core leaving behind the salt content. The modified Indian Ocean water within the core of

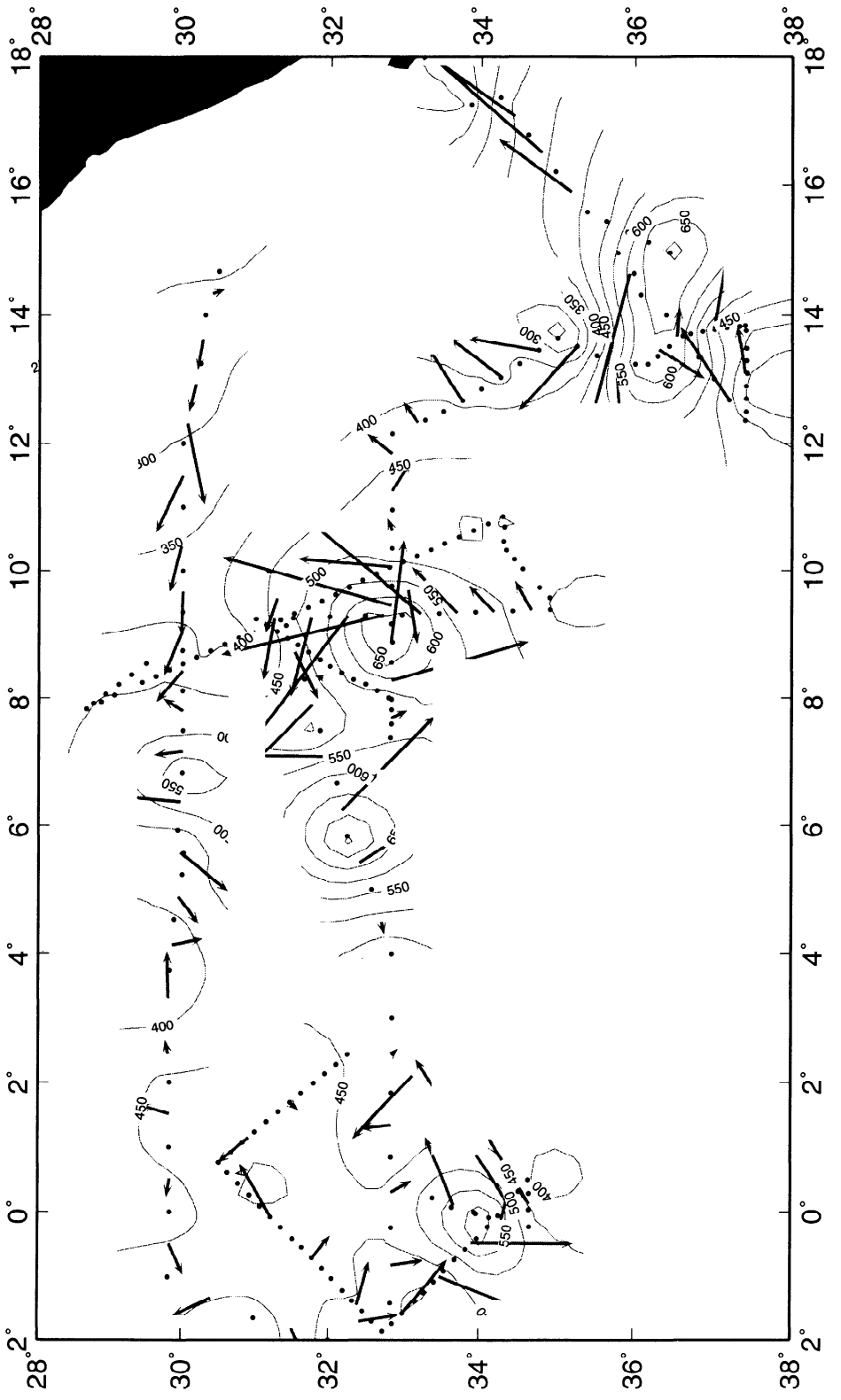

Figure 3. Contours of the depth of the 10°C isotherm (meters) with acoustic Doppler current profiler (ADCP) velocity vectors averaged between CTD stations (scale shown). Location of CTD and XBT stations are indicated by the circles.

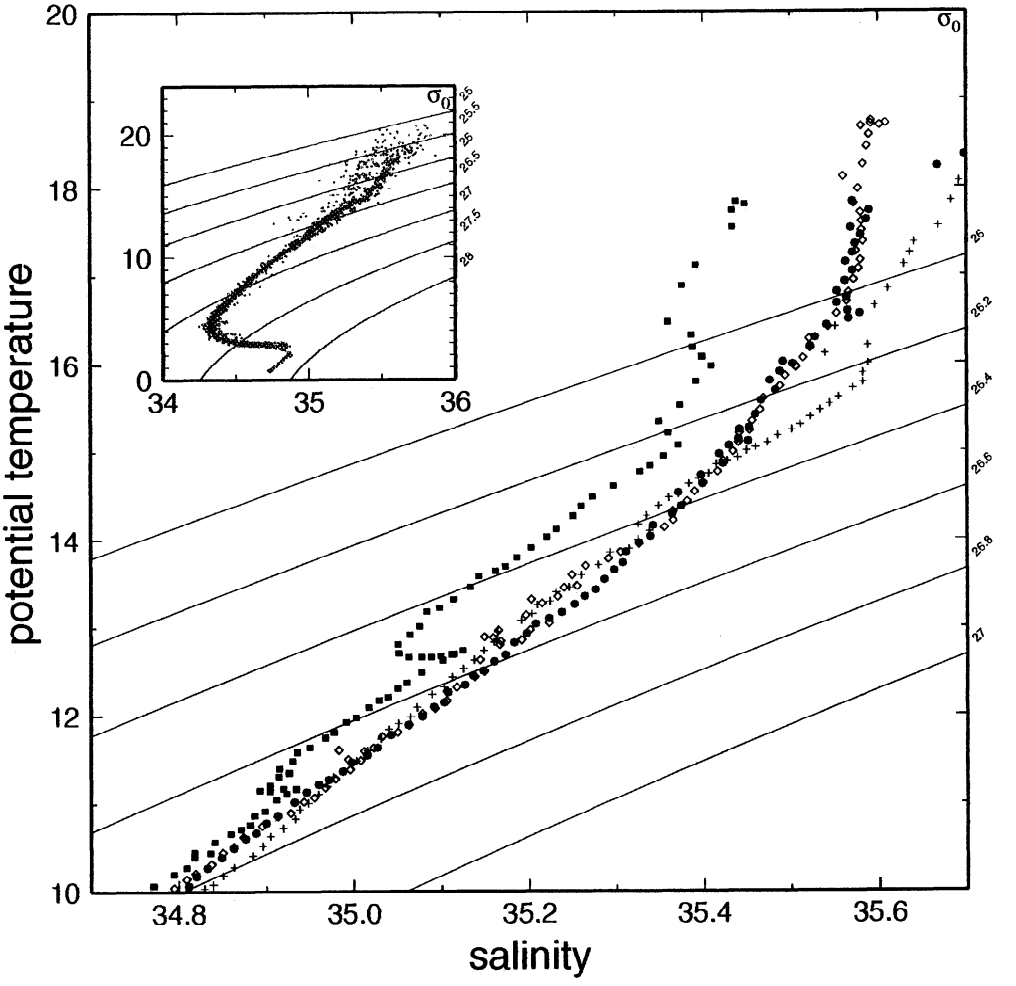

Figure 4. Potential temperature/salinity diagram for eddy 1 (squares, stations 30 and 31), eddy 2 (crosses, stations 35, 36, and 37), eddy 3 (circles, stations 53 and 54), and eddy 4 (diamonds, stations 66, 67, and 68).The inset shows the potential temperature/salinity diagram for the entire data set over the full range of values.

the eddy has the effect of adding salt to the 15-16°C layer of the South Atlantic. This eddy was not sufficiently well sampled to resolve the location of the center of the eddy, so the radial velocity profile could not be determined. The largest velocities that were observed with the ADCP (averaged over 15 min) at 250 m over this crossing of the eddy were 60 cm s^{-1}.

Another likely Agulhas Retroflection eddy, eddy 3 (Figure 1), was found just to the east at 9°E and 33°S. This eddy had a core temperature of about 17.5°C, with no positive salinity anomaly. The similarity of the temperature of the eddy core to the Agulhas Retroflection water indicates that this eddy has not experienced winter forcing. The zero crossing of the velocity for the east/west and north/south sections do not coincide. We estimated the location of the center of the eddy by bisecting the two chords and taking their point of intersection to be the center. The azimuthal velocities were computed for this choice for the center and smoothed with a 10-point running mean (Figure 6). It is not clear from Figure 6a at what radius the maximum velocity occurs; rather, there is a range of radii from about 40 to 75 km over which the velocities are indistinguishable. In an attempt to identify a radius of maximum velocity objectively, we assume geostrophic balance in the eddy and compute the pressure field

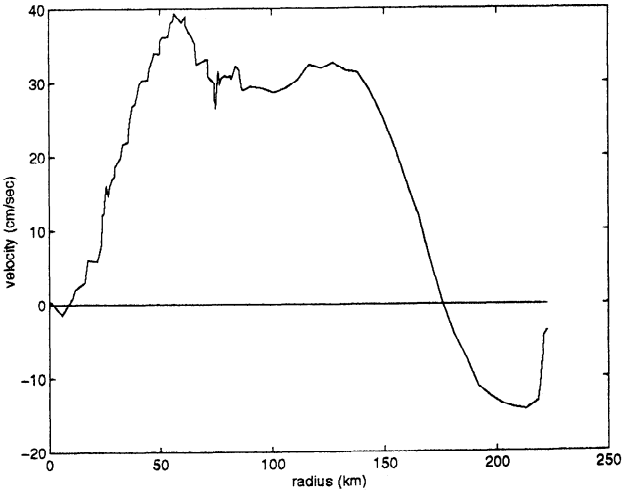

Figure 5. Azimuthal velocities (centimeters per second) around eddy 1 smoothed with a 10-point running mean versus radius (kilometers).

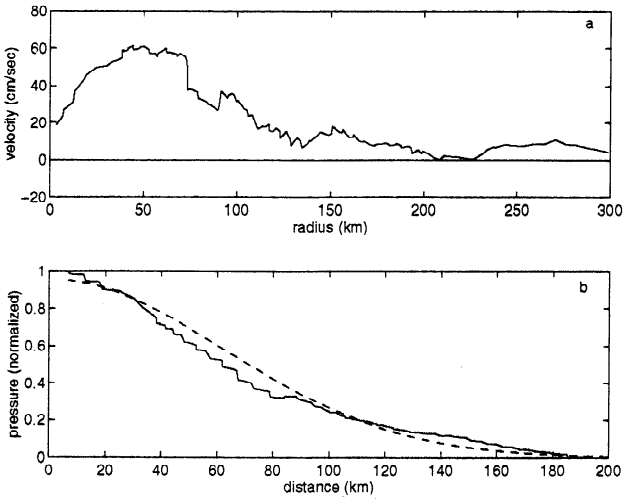

Figure 6. (a) Azimuthal velocities (centimeters per second) around eddy 3 smoothed with a 10-point running mean versus radius (kilometers). (b) Pressure field (normalized to the maximum value) computed from the integrated ADCP velocities, averaged over 15 min. (solid line) and with a Gaussian fit (dashed line).

from the integrated ADCP velocities (averaged over 15 min intervals) at 250 m (Figure 6b). We then fit a Gaussian curve,

$$P = P_0 exp(\frac{-r^2}{2L^2})$$

to the derived pressure field P from which we obtain the width of the Gaussian curve L which corresponds to the radius of maximum velocity. It should be noted that the value of L is fairly sensitive to the choice for the limit of integration which should be the horizontal extent of the eddy flow, so that the estimate of the radius of maximum velocity is not completely objective. We chose to start the integration at a radius of 200 km where the azimuthal velocities go to zero (Figure 6a). This gives a reasonable fit of a Gaussian curve to the calculated pressure field (Figure 6b). The resultant length scale L is approximately 60 km, and the unsmoothed azimuthal velocity at this radius is approximately 60 cm s^{-1}. This length scale is considerably smaller than what is commonly thought of as the horizontal scale of Agulhas eddies which is approximately 120 km [*Duncombe Rae*, 1991]. This result is discussed in section 3.

The proximity of the two Agulhas eddies, eddies 2 and 3, of different ages suggests that eddy 2 was being influenced by bottom topography (Figure 1 shows that the Walvis Ridge is west of the older eddy). Stalling of Agulhas eddies in the region of the Walvis Ridge has previously been observed using satellite-tracked drifters trapped within Agulhas eddies [*Olson and Evans*, 1986], as well as satellite altimeter data [*Byrne et al.*, 1995]. It is interesting, though, that eddy 2 is over a flat, deep part of the basin. We suggest that eddy 2 may have been deflected back to the east on encountering the Walvis Ridge. Such behavior has been demonstrated in a numerical model of the influence of bottom topography on Agulhas eddies [*Kamenkovich et al*, 1995]. They showed that for the case of a significantly barotropic eddy, as the modeled eddy approaches steep topography, it is deflected back toward the east, then travels west again [*Kamenkovich et al.*, 1995, Figure 7), and is almost completely destroyed before crossing the ridge. Eddy 2 may be responding to the presence of the Walvis Ridge in this way.

The fourth anticyclonic feature, eddy 4 (Figure 1), was centered at approximately 14°E and 36°S. It is elliptical in shape and is more vigorous than the other eddies, with maximum velocities of 80 cm s^{-1} typical of a newly formed eddy [*Olson*, 1991]. Because of the irregular sampling and the asymmetry of this eddy, the radius of maximum velocity could not be determined. The eddy core is the subtropical mode water of the Agulhas Retroflection (Figure 4). The location, the magnitude of the velocities, and the properties of the water in this eddy all indicate that this is a newly formed Agulhas eddy.

Although the circulation seems to be dominated by the eddy field in the sense that the most energetic currents in the region were in and around the eddies, there may be some robust large-scale circulation pattern induced by the interaction of the large-scale and eddy-scale flow fields. The vectors for the entire region shown in Figure 3 were averaged to reveal a net northward flow of 6.85 cm/s and a net westward flow of 0.75 cm s^{-1}. This shows the net movement of water out of this region at a depth of 250 m.

3. Comparison of ADCP and Hydrographic Data

Much of our present understanding of ocean circulation comes from flow fields derived from the geostrophic method. This method, however, provides limited information and is sometimes used in a manner that relies on rather tenuous reference layer assumptions. To convert to absolute velocity requires knowledge of the current at a specific depth, and as this is generally not available, oceanographers often resort to the assumption of a level of no motion as a reference for computing absolute velocities. Determining this level is by no means straightforward and is generally qualitative.

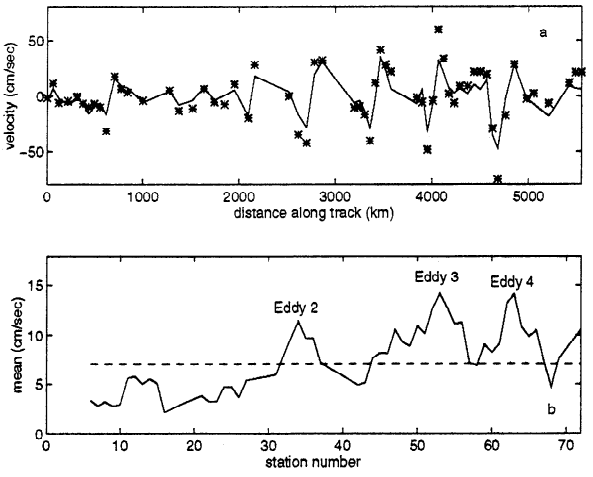

Figure 7. (a) Averaged across-track ADCP velocities at 250 m in centimeters per second (stars) and geostrophic velocities relative to 1500 dbar at 250 m (solid line) versus distance along the cruise track. Zero distance is at station 2 (Figure 1). (b) The smoothed (five-point running mean) differences in magnitude between ADCP cross-track and geostrophic velocities referenced to 1500 dbar (centimeters per second) plotted against station number. The 95% level of significance is indicated by the dashed line. The locations of the Agulhas eddies are annotated.

Specifying a level of no motion also precludes the presence of a barotropic component to the flow. The *Discovery* 202 ADCP and CTD data set is unique in that it allows for comparison of the derived geostrophic velocities with measured velocities. This comparison may shed some light on how well the derived geostrophic velocities reconstruct the actual flow field.

In order to compare the measured with the geostrophic velocities, the ADCP velocities at 250 m are averaged between stations (averaging approximately 6 hours temporally and 100 km spatially) and decomposed into along- and across-track velocities. This depth was chosen because it was presumably below the layer affected by wind-induced surface processes and where the ADCP quality was still high. The across-track component and geostrophic velocities relative to a level of no motion at 1500 dbar for each station pair are shown in Figure 7a. Because we are interested in flows that are in geostrophic balance, it is necessary to account for processes that occur on shorter timescales that affect both estimates of the velocity, i.e., geophysical noise. For the ADCP velocities the effect of the highest-frequency phenomena is presumably removed through averaging. There remains, however, transient currents that occur over the range of periods between 6 hours and a few days, in particular, tides and internal waves which have periods of 12 and 24 hours. These phenomena are expected to have higher amplitudes in the upper layer which would bias the current measured by the ADCP (at 250 m) relative to the geostrophic velocities referenced to 1500 dbar. Because the *Discovery* 202 data set was not designed to investigate how transient currents affect measured velocities and CTD data, we attempt to account for these flows by estimating their magnitude from current meter mooring (CMM) data that were collected on the first and third legs of the BEST project [*Pillsbury et al.*, 1994]. The frequency spectrum (not shown) of the velocities from CMM - 4 (see Figure 1 for CMM - 4 location) from a depth of 210 m shows significant peaks at 12 and 24 hours, while the rest of the spectrum is more or less red. The time series was filtered with a passband from 10 to 30 hours, and the resultant time series had a mean magnitude of 5 cm/s [C. Duncombe Rae, personal communication, 1995]. We interpret this as a rough estimate of the magnitude of the inertial and tidal flows in this region. This value is consistent with the one found by *Saunders and King* [1995], who used data from long-period stations and estimates of tidal motions from *Schwiderski* [1979]. Because the magnitude of the geophysical noise is considerably larger than the instrumental noise for the ADCP (1-2 cm s^{-1}), we consider only the contribution of the former to the noise in the ADCP velocities, which presents a potential bias of 5 cm s^{-1}.

Determining how the density field is affected by the inertial and tidal flows is more complicated due to the distribution in time and space of the CTD casts. We propose a somewhat ad hoc method of evaluating this using inverted echo sounder (IES) data from the other BEST cruises. The variability of the depth of the 10° isotherm Z_{10} can be inferred from the IES records of the acoustic travel time [*Duncombe Rae et al*, 1995). The sampling interval was 1 hour for the IES. We computed the standard deviation of 10-hour averages of the depth of the 10° isotherm measured at SN58 (see Figure 1 for SN58 location), which was found to be an average of 27 m for the entire time series (18 months). We interpret this as a measure of the variability that the density profile undergoes between the starting time of the first of a pair of stations and the time the second station is completed (10 hours, on average, for the *Discovery* 202 cruise). We assume that this variability is random and compute the resulting error in the geostrophic calculation for two hypothetical stations separated by 100 km (the mean spacing between CTDs for the *Discovery* 202 cruise). We generate two records of the 10° isotherm depth of randomly distributed noise with a mean of zero and standard deviation of 27 m. The geostrophic velocities are calculated from the following relationz;

$$fv_g = g' \frac{\partial Z_{10}}{\partial r}$$

where v_g is the geostrophic velocity, f is the Coriolis parameter, dr is the distance between the stations (100 km), and g' = 0.0134 m s^{-1} and is the coefficient of the linear regression between Z_{10} and the dynamic height relative to 1800 dbar (Duncombe Rae et al., submitted manuscript, 1995). The standard deviation in the velocities was found to be about 1 cm s^{-1}. We take this to be an estimate of the potential error in the geostrophic velocities computed from CTD data that are spaced 6 hours (100 km) apart owing to geophysical noise. Note that this assumes that the error at the two hypothetical stations is uncorrelated.

In summary, the ADCP velocities have a potential bias from tidal and inertial flows of 5 cm/s and the variability in the density field over 6 hours can give rise to a standard deviation in the geostrophic velocities as large as 1 cm s^{-1} which corresponds to an error of +/-2 cm s^{-1} at the 95% confidence level. In comparing these two estimates of the velocity therefore, differences between them must be larger than 7 cm s^{-1} to be significantly different from zero at the 95% confidence level.

The correlation coefficient between the ADCP cross-track velocity and the geostrophic velocities relative to 1500 dbar (both at 250 m) was found to be 0.93 along the entire cruise track. This correlation was also done for geostrophic velocities referenced to 1000 dbar and yielded almost the same correlation coefficient (0.91). This implies that use of the 1500-dbar level as a reference resolves the baroclinic field. Although there is a high linear correlation between the ADCP cross-track and geostrophic velocities, there is some discrepancy between the magnitudes of the velocities (Figure 7a). The individual differences for each station pair, as well as the error estimates, were smoothed with a five-point running mean and are shown in Figure 7b. This plot is characterized by several peaks, each of which corresponds to the locations of the three Agulhas eddies.

The highest peaks are centered at eddies 2, 3 and 4. Such discrepancies in the velocities may arise from either ageostrophic (nonlinear) flow, barotropic flow, or unresolved baroclinic flow. We do not expect the latter to be important, as the baroclinic field is well resolved by using the 1500-dbar level as a reference. Previous studies using observations of both Agulhas Retroflection and Gulf Stream eddies [*Olson and Evans*, 1986; *Olson et al.*, 1985], as well as numerical models of Agulhas eddies [*Chassignet et al.*, 1990], imply that the eddies have a significant barotropic component near the eddy centers. *Saunders and King* [1995], on the other hand, claim that the differences they observed between ADCP and geostrophic velocities referenced to 4000 dbar within eddies is due to ageostrophic flow. We have chosen to look in more detail at eddy 3, the Agulhas eddy that was the most

wellsampled, to investigate the cause of the differences between measured and derived baroclinic velocities in the eddies surveyed during *Discovery* cruise 202.

The magnitude of the ageostrophic flow due to the curvature terms in the radial equation of motion for an axially symmetric eddy,

$$\frac{v^2}{r} + fv = \frac{1}{\rho}\frac{\partial P}{\partial r} = fv_g$$

where v is the total flow and v_g is the geostrophic flow, can be compared with the geostrophic flow by the following relation:

$$v - v_g = \frac{v^2}{fr}.$$

We computed the value of v^2/fr using the azimuthal ADCP velocities averaged over 15-min intervals, and then, to compare this with the geostrophic velocities, the term v^2/fr was averaged between CTD stations. The result is shown in Figures 8b and 9b (dashed lines, circles) for the east/west and north/south crossings of eddy 3, respectively. The difference between the ADCP cross-track velocities averaged between CTD stations and the geostrophic velocities relative to a flat geopotential surface at 1500 dbar are also shown in Figures 8b and 9b (solid lines, stars). This difference is as much as 3 times larger than the expected nonlinear flow (v^2/fr) at a radius of about 50 km (Figure 8b) and is still large at radii greater than 100 km. We conclude that the difference between the averaged ADCP and the baroclinic geostrophic velocities is due, at least in part, to a barotropic component of the flow manifesting in a nonzero velocity at 1500 db. For the north/south crossing of the eddy (Figure 9b) the differences are not as significant at similar radii, and v^2/fr becomes very large near the center. *Saunders and King* [1995] encountered

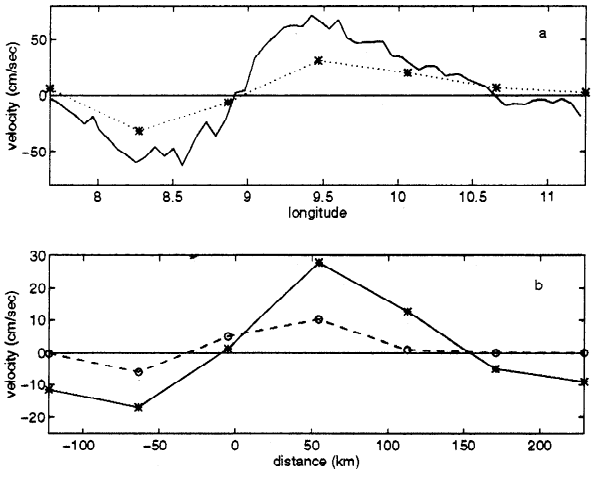

Figure 8. (a) The 15-minute averaged ADCP velocities in centimeters per second (solid), and geostrophic velocities relative to 1500 dbar (stars, dotted line) versus longitude in the east/west crossing of eddy 3 . Positive values are to the north. (b) Differences between the ADCP velocities averaged between CTD stations in centimeters per second (solid line, stars), and v^2/fr in centimeters per second, the expected nonlinear flow, averaged between stations where v is the ADCP velocity (dashed line, circles) versus distance from the location of the change in sign of velocities.

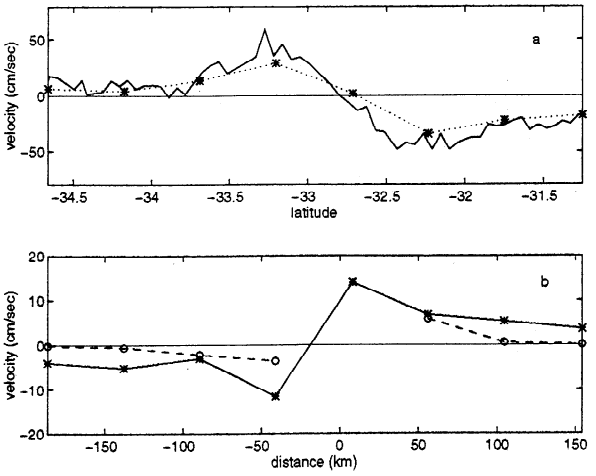

Figure 9. Same as Figure 8, but for the north/south crossing of eddy 3. Note that v^2/fr is not shown at the radius near zero. This is because the value was extremely large at that point.

the same eddy on a previous cruise. They found differences between the ADCP data and the geostrophic velocities referenced to 4000 dbar, and by calculating the contribution of the curvature term in an analogous way to the argument given here, they interpret the difference as the result of ageostrophic flow. They use a radius of curvature of 1/30 km^{-1} and a total velocity of 1 m s^{-1} to show that the geostrophic flow is only 67% of the total flow. Such large velocities, however, were not observed in this eddy during the *Discovery* 202 cruise (the largest instantaneous azimuthal velocities were 60 cm s^{-1} which occur at a radius of approximately 60 km). We do not exclude the possibility that there is ageostrophic flow in eddy 3. In fact, in the north/south crossing of eddy 3 the magnitude of v^2/fr was as large as the differences between the ADCP and geostrophic velocities. However, there remains some flow measured by the ADCP that cannot be explained by the geostrophic and nonlinear flow, and this is what we interpret as a barotropic component to the flow in eddy 3. The magnitude of this flow, as large as 15-25 cm s^{-1}, is consistent with, though slightly larger than , the 15 cm s^{-1} that *Chassignet et al.* [1990] find for the barotropic flow in their numerical model.

Additional evidence that Agulhas eddies are significantly barotropic comes from the observation that their paths respond to bottom topography, in particular, to the Walvis Ridge [*Olson and Evans*, 1986; *Byrne et al.*, 1995]. As was mentioned before, the proximity of the two Agulhas eddies at least a year apart in age suggests that the older eddy was being stalled by the Walvis Ridge. In their numerical models, *Smith and O'Brien* [1983] and *Kamenkovich et al.* [1995] find that upper ocean eddies are not affected by bottom topography. Only when there is a significant barotropic flow within the eddies do they feel the bottom, which seems to be the case for the Agulhas eddies surveyed during *Discovery* cruise 202, as well as in previous studies [*Olson and Evans*, 1986].

It is common practice to use the radius of maximum velocity of an eddy as its horizontal length scale. The length scale found for eddy 3 was approximately 60 km (Figure 6b). The total velocity field is the sum of the contributions from the density field (the baroclinic flow) and the sea surface elevation (the barotropic flow). For eddy 3 the radial profile of the 10^{o} isotherm is shown in Figure 10. The maximum gradient of the

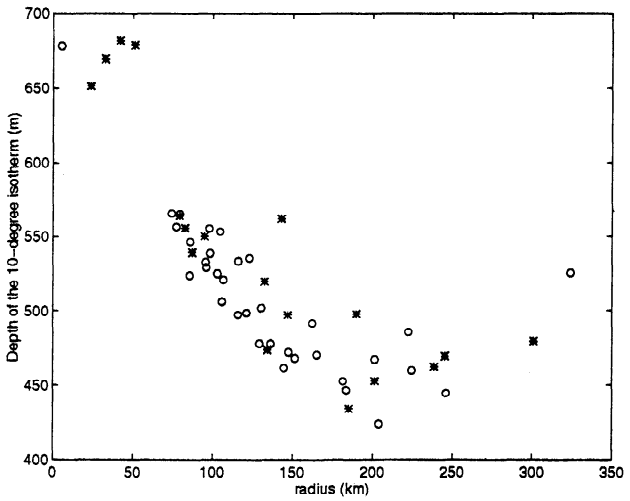

Figure 10. Depth of the 10° isotherm in eddy 3 (meters) versus radius (kilometers). CTD measurements are indicated by stars and the XBTs, by circles.

thermal field occurs between 50 and 75 km. This implies that the form of the radial profile of the total velocity in eddy 3 is consistent with the baroclinic field. There was not sufficient resolution of the density field from the CTDs to determine the form of the barotropic flow. The relatively small length scale of Eddy 3 is due to the steep gradient of the thermal field outside the core of the eddy. This does not seem to be a typical feature of Agulhas eddies. However, use of the ADCP underway facilitated the determining of the center of the eddy, which allowed for better sampling of the thermal field near the eddy core.

4. Total Geostrophic Velocities and Transports

One of the main attributes of ADCP data is that it can be used in combination with hydrographic data to yield a total geostrophic flow field which incorporates both the baroclinic and barotropic flow. Total geostrophic velocities were computed relative to a level of known motion at 250 m taken to be the averaged ADCP velocities. From this the total transport of water in the Benguela Current was calculated for the section along 30°S. This constrains the amount of water transported out of the region to the north. Also, the total transport of water in the eddies was computed in order to estimate the contribution of Agulhas eddies to the input of Indian Ocean water into the Atlantic.

ADCP referenced geostrophic transport for the upper kilometer across the 30°S section is 25 Sv toward the north. S.L. Garzoli and A.L. Gordon (Origins and variability of the Benguela Current, submitted to *Journal of Geophysical Research*, 1995) suggest that this transport is near the maximum encountered during the BEST experiment. *Stramma and Peterson* [1989] found a similar value of 21 Sv across a 32°S section for the upper layer flow for the geostrophic flow referenced to s_0=27.75 kg m^{-3}, which they call the Benguela Current. The ADCP referenced transport of water warmer than 9°C across 30°S is 17 Sv toward the north. Again, this compares favorably with previous estimates of the transport for that section relative to a zero-velocity surface at 1500 dbar which range from 14 to 16 Sv [*Gordon et al.*, 1987, 1992]. These results suggests that the transport of the Benguela Current in the upper 1000 m along this section is dominated by the baroclinic field. The ratio of the transport relative to a zero velocity surface at 1500 dbar to the ADCP referenced geostrophic transport for the upper kilometer was 0.92, and for water warmer than 9°C it was 0.88. That is, about 90% of the flow is baroclinic in the upper layers. On the other hand, the ADCP referenced transport of the entire water column (going to the deepest common depth between stations) across the 30°S section was found to be 70 Sv toward the north. We do not suggest that this is a realistic value for the large-scale transport across this section. Rather, this result could arise because the ADCP velocities in this section of weaker flow (relative to the eddy flows) may be biased by high-frequency barotropic events and transient processes such as tides and inertial currents. These velocities, when integrated over the entire water column, overwhelm the climatic transport. Thus, in regions of weaker flow where transient processes may have a magnitude comparable to that of the geostrophic flow, i.e., a low signal-to-noise ratio, the use of ADCP velocities as a reference for geostrophic calculations should be considered more carefully. The total transport (down to the deepest common depth between stations) relative to a zero-velocity surface at 1500 dbar was found to be 12 Sv. As the ADCP referenced transport for the upper kilometer is 25 Sv, this implies that there is 9 Sv of the southward transport at depths greater than 1 km. This is probably a more realistic representation of the climatic mean flow for the entire water column across this section.

The total transport for eddy 3 (note that this was the only eddy with sufficient CTD coverage for such analysis) was also calculated based on the ADCP referenced geostrophic velocities. The ADCP referenced volume transport above 1500 m was found to be 51 Sv, while the transport relative to a zero-velocity surface at 1500 m was 27 Sv. Thus the ratio of baroclinic to total flow in this eddy is approximately 0.5 (only 50% of the flow was barotropic). A transport of 51 Sv for eddy 3 is larger than previous estimates of the baroclinic geostrophic transport for different Agulhas eddies in this region, which range from 15 to 40 Sv [*McCartney and Woodgate-Jones*, 1991].

It is desirable to determine the amount of Indian Ocean water trapped within these eddies, as this is one of the mechanisms of the interocean transport which affects the properties of the South Atlantic. Previous estimates of this transport of Indian Ocean water by Agulhas eddies range between 0.4 and 1.1 Sv per eddy [*McCartney and Woodgate-Jones*, 1991], an average value of 1.7 Sv for three different eddies [*Byrne et al.*, 1995], and 1.05 and 1.25 (above the 10° and 8° isotherms, respectively) [*van Ballegoyen et al.*, 1994]. The method used in these studies and which will be used here is based on a study done by *Flierl* [1981]. The upper limit to the trapping area of Indian Ocean water within the eddy is defined by the region where the parameter ε, the ratio of the maximum azimuthal velocity at a particular depth to the translation speed of the eddy, is greater than 1. Using this method, we find a transport of 0.45 to 0.90 Sv (drift speeds of 10 and 5 cm s^{-1}, respectively) for the upper 1500 dbar in eddy 3. The CTDs for the eddy component of *Discovery* cruise 202 only went to a depth of 1500 dbar, so the transport in the lower layers could not be determined. It is, however, the thermocline and

intermediate waters that are expected to have the largest effect on the salt budget of the South Atlantic [*Gordon et al.*, 1992], so that the transport values for the upper 1500 dbar are the relevant ones. These estimates are largely consistent with previous ones using the same method. If the frequency of Agulhas eddy shedding is six per year [*van Ballegoyen et al.*, 1994], this would result in a transport of 2.7 to 5.4 Sv of Indian Ocean water by Agulhas eddies, which represents about 20-30% of the 15 Sv for Indian to South Atlantic transport predicted by *Gordon* [1985].

5. Energy Calculations for Eddy 3

We used the method of *Olson and Evans* [1986] to calculate the available potential energy (APE) and kinetic energy (KE) of eddy 3. These quantities were calculated in the following way:

$$\mathrm{APE} = \frac{\rho g'}{2} \int_A [Z_{10} - (Z_{10})_\infty]^2 \, dA$$

$$\mathrm{KE} = \frac{\rho}{2} \int_V v^2 \, dV$$

where Z_{10} is the 10°C isotherm depth, $(Z_{10})_\infty$ is the background 10°C isotherm depth outside the influence of the ring, g' was defined in section 3 and is taken as 0.0134 m s^{-1}. The integrations are over A, the horizontal area of the eddy, and V, the volume of the eddy above the 10°C isotherm. The horizontal extent of the eddy was taken to be at a radius of 200 km, where Figure 6a shows that the azimuthal velocities in the eddy go to zero, and the value of $(Z_{10})_\infty$ was taken as the depth of the 10°C isotherm at that radius (approximately 450 m). The calculations were done for the layer above the 10°C isotherm in order to compare them with previous estimates. The results are shown in Table 1 and are compared with values for eddies from the other BEST cruises [*Duncombe Rae et al.*, 1995] and from other Agulhas eddies discussed by *Olson and Evans* [1986] and *Byrne et al.* [1995]. The KE was calculated using both the baroclinic and total (baroclinic plus barotropic) geostrophic velocities. Including the barotropic flow has no effect on the calculation of the APE but almost doubles the KE. Although the total KE is approximately the same magnitude as the baroclinic KE for the two eddies discussed by *Olson and Evans* [1986], it is much larger than the baroclinic KE for the eddies surveyed during the BEST experiment and those studied by *Byrne et al.* [1995]. Of note is the partitioning of total mechanical energy between the APE and the KE; when the barotropic flow is included in the calculation of KE, the APE and KE are about equal, while previous calculations using only the baroclinic showed the APE to be up to 8 times larger than the KE.

Table 1. Energy calculations for Agulhas Eddies

	APE*, x10^{15} J	KE, x10^{15} J	
		Baroclinic only†	Total‡
Eddy 3	7.0	4.0	7.0
B1-1	17.4	2.3	
OE1	51.4	8.7	
OE2	30.5	6.2	
Average	18	4.5	

Eddy 3 is from this study. B1-1 is an Agulhas eddy from the Benguela Source and Transport Project (BEST) 1 cruise discussed by *Duncombe Rae et al.* [1995]. OE1 and OE2 are an Agulhas and Capetown eddy, respectively, discussed by *Olson and Evans* [1986]. Average refers to an average of 12 Agulhas eddies from *Byrne et. al.* [1995].

*Available potential energy (APE) and Kinetic energy (KE) were calculated above the 10°C isotherm.

†Values were calculated from geostrophic velocities relative to a level of no motion at 1500 dbar.

‡Value was calculated from the geostrophic velocity referenced to averaged ADCP velocities at 250 m (see Section 4).

6. Discussion

Because of the sparsity of direct current measurements, often only the baroclinic component of geostrophic flows as revealed by more traditional "dynamical" methods has been studied. Analysis of the *Discovery* cruise 202 data set reveals that the Benguela Current across the 30°S section is dominated by the baroclinic field, while the eddy features within the current are significantly barotropic. It is unclear what the origin of the barotropic flow in Agulhas eddies is. Furthermore, it is not obvious that the eddies should maintain a barotropic flow. Using a two-layer model, *McWilliams and Flierl* [1979] and *Meid and Lindemann* [1979] show that an eddy that initially has coherent flow in the upper and lower layers will rapidly reach a state of deep compensation where the flow in the lower layer is out of phase with that of the upper layer. *Kamenkovich et al.* [1995] have attempted to address the issue of the evolution of the vertical structure of Agulhas eddies using a two-layer model. They find that the amount of compensation that takes place within the eddies depends on the horizontal scale of the eddy relative to the Rossby radius of deformation. However, the horizontal scale of the eddy for which an initially coherent eddy will remain so (110-120 km) in their study is much larger than that of eddy 3. It thus remains unclear as to why Agulhas eddies maintain a significant barotropic flow.

The presence of barotropic flow in Agulhas eddies may influence their evolution and trajectories within the South Atlantic [*Smith and O'Brien*, 1983; *Kamenkovich et al.*, 1995]. The behavior of a significantly barotropic eddy in the vicinity of the Walvis ridge in the modeling study of *Kamenkovich et al.* [1995] (see section 2) and the presumed behavior of eddy 2 may illustrate the fate of some Agulhas eddies, while others have been observed as far west as the eastern side of the Mid-Atlantic Ridge [*McCartney and Woodgate-Jones*, 1991]. The effect of the barotropic component on Agulhas eddies would, in turn, influence where the Indian Ocean water is introduced into the South Atlantic. The adjusted steric anomaly map of *Reid* [1989], which depicts the absolute circulation field, shows water from the eastern South Atlantic flowing northward. *Gordon* [1986] suggests that some of this water continues across the equator to ultimately affect the formation of North Atlantic Deep Water. Alternatively, the eddies that succeed in traversing the Walvis Ridge travel into the subtropical gyre of the South Atlantic [see *Byrne et al.*, 1995, figure 4], where the water they carry

with them would be deposited as the eddy decays. In summary, consideration of the barotropic flow in Agulhas eddies is important in understanding the basic structure and behavior of Agulhas eddies and the role of these eddies in the Indian-South Atlantic link in global thermohaline circulation.

A more detailed picture of the dynamical processes in the source region of the Benguela Current emerges from the *Discovery* cruise 202 data set. In particular, the combination of hydrographic data and ADCP data reveals information about the basic structure of Agulhas eddies, including a possible barotropic component, smaller horizontal length scale, and different partitioning of total mechanical energy , which is important in modeling these eddies. Although this is only a snapshot view of the circulation in the source region of the Benguela Current and may not be representative of the mean circulation pattern in that region, the dynamical processes that occur there are well documented by this data set. Use of satellite altimeter data, as well as the data collected from the current meter moorings during the other legs of the BEST project, in conjunction with the *Discovery* cruise 202 data set may serve to determine how representative this picture is of the circulation in this region. Such future efforts may provide information about the interannual variability of transport of mass and energy from the Indian Ocean into the South Atlantic.

Acknowledgments. The authors would like to thank Vladimir Kamenkovich, Donald Olson, Yochanan Kushnir, Chris Duncombe Rae, Dierdre Byrne, and Bruce Huber for their helpful input. We gratefully acknowledge the assistance of the officers and crew aboard *Discovery* cruise 202 and Andrew Cormack for his help in processing the ADCP data. Financial support for this work came from OCE grant 91-02722. This is a Lamont-Doherty Earth Observatory contribution 5406.

References

Byrne, D.A., A.L. Gordon, and W.F. Haxby, Agulhas Eddies: A synoptic view using Geosat ERM data, *J. Phys. Oceanogr., 25,* 902-917, 1995.

Chassignet, E.P., D.B. Olson, and D.B. Boudra, Motion and evolution of oceanic rings in a numerical model and in observations, *J. Geophys. Res., 95,* 22,121-22,140, 1990.

Duncombe Rae, C.M., Agulhas Retroflection rings in the South Atlantic Ocean, *S. Afr. J. Mar. Sci., 11,* 327-344, 1991.

Duncombe Rae, C.M., S.L. Garzoli, and A.L. Gordon, The Eddy Field of the South-East Atlantic Ocean: A Statistical Census from the BEST Project, *J. Geophys. Res.,* in press, 1995.

Feron, R.C.V., W.P.M. De Ruijter, and D. Oskam, Ring shedding in the Agulhas Current system, *J. Geophys. Res., 97,* 9467-9477, 1992.

Flierl, G.R., Particle motions in large-amplitude wave fields, *Geophys. Astrophys. Fluid Dyn., 18,* 39-74, 1981.

Gordon, A.L., Indian-Atlantic transfer of thermocline water at the Agulhas Retroflection, *Science, 227,* 1030-1033, 1985.

Gordon, A.L., Interocean exchange of thermocline water, *J. Geophys. Res., 91,* 5037-5046, 1986.

Gordon, A.L., and W.F. Haxby, Agulhas eddies invade the South Atlantic: Evidence from Geosat altimeter and shipboard conductivity-temperature-depth survey, *J. Geophys. Res., 95,* 3117-3125, 1990.

Gordon, A.L., J.R.E. Lutjeharms, and M.L. Grundlingh, Stratification and circulation at the Agulhas Retroflection, *Deep Sea Res., Part A, 34,* 565-599, 1987.

Gordon.A.L., R.F. Weiss, W.M. Smethie, and M.J. Warner, Thermocline and intermediate water communication between the South Atlantic and Indian Ocean, *J. Geophys. Res., 97,* 7223-7240, 1992.

Kamenkovich, V.M., Y.P. Leonov, D.A. Nechaev, D.A. Byrne, and A.L. Gordon, On the influence of bottom topography on the Agulhas Eddy, *J. Phys. Oceanogr.*, in press, 1995.

Lutjeharms, J.R.E., and J. Cooper, Inter-basin leakage through Agulhas Current Filaments, *Deep Sea Res.*, Part A, in press, 1995.

Lutjeharms, J.R.E., and R.C. van Ballegooyen, The retroflection of the Agulhas Current, *J. Phys. Oceanogr., 18,* 1570-1583, 1988.

McCartney, M.S., and M.E. Woodgate-Jones, A deep-reaching anticyclonic eddy in the Subtropical Gyre of the eastern South Atlantic, *Deep Sea Res., Part A, 38,* 411-443, 1991.

McWilliams, J.C., and G. Flierl, On the evolution of isolated non-linear vortices, with application to Gulf Stream rings, *J. Phys. Oceanogr., 9,* 213-230, 1979.

Meid, R.P., and G.L. Lindemann, The propogation and evolution of cyclonic Gulf Stream rings, *J. Phys. Oceanogr., 9,* 1183-1206, 1979.

Olson, D.B., Rings in the ocean, *Annu. Rev. Earth Planet Sci., 19,* 283-311, 1991.

Olson, D.B., and R.H. Evans, Rings of the Agulhas Current, *Deep Sea Res., Part A, 33,* 27-42, 1986.

Olson, D.B., R.W. Schmitt, M. Kennelly, and T.M. Joyce, A two-layer diagnostic model of the long-term physical evolution of warm core ring 82B, *J. Geophys. Res., 90,* 8813-8822, 1985.

Olson, D.B., R.Fine, and A.L. Gordon, Convective modification of water masses in the Agulhas, *Deep Sea Res.., Part A, 39,* S163-S181, 1992.

Pillsbury, R.D., J.M. Bottero, G. Pittock, D.C. Root, J. Simkins III, and R.E. Still, Benguela Source and Transport Project (BEST): Current Measurements off the Coast of South Africa, *Data Report 157, Reference 94-3,* WOCE ACM-4, June 1992- October 1993, Natl. Sci. Found., Washington, D.C., 1994.

Reid, J.L., On the total geostrophic circulation of the South Atlantic Ocean: Flow patterns, tracers and transports, *Prog. Oceanogr., 23,* 149-244, 1989.

Saunders, P.M., and B.A. King, Bottom current derived from a shipborne ADCP on WOCE Cruise A11 in the South Atlantic, *J. Phys. Oceanogr., 25,* 329-347, 1995.

Schwiderski, E.W., Global ocean tides, 2, The semidiurnal principal lunar tide (M2) in *Atlas of Tidal Charts and Maps, NSWC Publ. TR 79-414,* 90 pp, Nav. Surface Weapons Cent., Dahlgreen, Va., 1979.

Shannon, L.V., J.R.E. Lutjeharms, and J.J. Agenbag, Episodic input of subantarctic water into the Benguela Current region, *S. Afr. J. Sci., 8,* 317-322, 1989.

Smith, D.C., IV, and J.J. O'Brien, The interaction of a two-layer isolated mesoscale eddy with bottom topography, *J. Phys. Oceanogr., 13,* 1681-1697, 1983.

Smythe-Wright, D., A.L. Gordon, and P. Chapman, CFC-113 shows Brazil Current Rings Crossing the South Atlantic to the Agulhas Retroflection Region, *J. Geophys. Res.*, in press, 1995.

Stramma, L., and R.G. Peterson, Geostrophic transport in the Benguela Current Region, *J. Phys. Oceanogr., 19,* 1440-1448, 1989.

Stramma, L., and R.G. Peterson, The South Atlantic Current, *J. Phys. Oceanogr., 20,* 846-859, 1990.

van Ballegooyen, R.C., M.L. Grundlingh, and J.R.E. Lutjeharms, Eddy fluxes of heat and salt from the southwest Indian Ocean into the southeast Atlantic Ocean: A case study, *J. Geophys. Res., 99,* 14,053-14,070, 1994.

Walker, N.D., and R.D. Mey, Ocean-atmosphere heat fluxes within the Agulhas Retroflection region, *J. Geophys. Res., 93,* 15,473-15,483, 1988.

Amy C. Clement and Arnold L. Gordon, Lamont-Doherty Earth Observatory, P. O. Box 1000, Route 9W, Palisades, NY 10964-8000. (e-mail: hhellmer@lamont.ldeo.columbia.edu; sjacobs@lamont.ldeo.columbia.edu)

(Received October 3, 1994; revised July 3, 1995;
accepted August 4, 1995.)